

## Miscibility and Properties of Ethyl-Branched Polyethylene/Ethylene-Propylene Rubber Blends (II)

Ur-Ryong Cho

Department of Applied Chemical Eng., Korea Univ. of Technology and Education, Chonan 330-708, Korea

(Received July 21, 2001, Revised April 9, 2002, Accepted April 12, 2002)

### 에틸 가지화된 폴리에틸렌과 에틸렌-프로필렌 고무 블렌드의 혼화성과 물성(II)

조을룡

한국기술교육대학교 응용화학공학과

(2001년 7월 21일 접수, 2002년 4월 9일 수정, 2002년 4월 12일 채택)

**ABSTRACT** : Ethyl-branched polyethylene [PE(2)] containing 2mole% ethyl branch and three ethylene-propylene rubbers (EPR's) having the same ethylene(E)-propylene(P) molar ratio(E/P=50/50) with different stereoregularity, that is, random EPR (r-EPR), alternating-EPR (alt-EPR) and isotactic-alternating-EPR (iso-alt-EPR) were mixed for the investigation of their properties depending on the stereoregularity. Crystallinity of the prepared blends decreased with increasing content of amorphous EPR because of a decrease in both the degree of annealing and kinetics of diffusion of the crystallizable polymer content. With blend composition, crystallinity was reduced with the stereoregularity in EPR. The thermodynamic interaction parameter( $\chi$ ) for the three blend systems approximately equals to zero near the melting point. These systems were determined to be miscible on a molecular scale near or above the crystalline melting point of the crystalline PE(2). From the measurement of  $T_m$  vs.  $T_c$ , the behavior of PE(2) is mainly due to a diluent effect of EPR component. The spherulite size measured by small angle light scattering (SALS) technique depended upon blend composition, and stereoregularity of EPR. The size of spherulite was enlarged with the content of rubbery EPR and the decrease of stereoregularity in EPR.

요약 : 2몰% 에틸가지를 포함하는 에틸 가지화 폴리에틸렌[PE(2)]과 에틸렌-프로필렌 몰비가 50:50 으로 같지만 입체규칙성이 다른 랜덤-에틸렌-프로필렌 고무(r-EPR), 교호-에틸렌-프로필렌 고무(alt-EPR) 및 이소탁틱-교호-에틸렌-프로필렌 고무(iso-alt-EPR)를 에틸렌-프로필렌 고무를 입체규칙성의 차이에 대한 혼화성과 물성의 차이를 조사하기 위하여 혼합하였다. 혼합된 블렌드의 결정화도는 고무상 EPR 성분의 증가에 따라 감소되었으며, EPR의 입체규칙성이 작을수록, 혼합 조성의 증가할수록 감소하였다. 열역학적 interaction parameter( $\chi$ ) 값은 3가지 블렌드 모두 거의 영에 가까운 값을 나타내어 본 블렌드계는 PE(2)의 녹는점 가까이 또는 그 이상에서 상호간 섞일 것으로 판단되었다. 녹는점( $T_m$ )과 결정화온도( $T_c$ )의 측정에서부터 세가지 블렌드는 혼합조성과 입체규칙성에 관계없이 직선관계를 보여주어 이 블렌드계의 PE(2)의 용융거동은 주로 희석효과(diluent effect)에 기인함을 알 수 있었다. Small angle light scattering(SALS) 방법에 의한 PE(2)의 spherulite의 크기는 세가지 블렌드계가 EPR의 혼합비 증가에 따라 증가하였으며, 같은 혼합비에서는 r-EPR>alt-EPR>iso-alt-EPR> 순서로 증가하였다.

*Keywords* : crystallinity, interaction parameter, diluent effect, spherulite size

†대표저자(e-mail : urcho@kut.ac.kr)

## I. Introduction

In the previous paper<sup>1</sup>, the three binary blend mixtures of polyethylene [PE(2)] having 2mole% ethyl branch and three different ethylene-propylene rubbers (EPR's) possessing the same ethylene(E)-propylene(P) molar ratio (E/P=50/50) with different stereoregularity, namely, random EPR (r-EPR), alternating-EPR (alt-EPR) and isotactic-alternating-EPR (iso-alt-EPR) were investigated to study on melting point of blends, d-spacings of crystal structure, density behavior, stress-strain behavior, glass transition temperature, and so on. We have found that blends of crystalline polymer with a rubbery polymer showed some interesting phenomena on final physical properties of the mixtures<sup>2-5</sup>. From the first observation of the three PE(2)/EPR blends, the melting point depression of polyethylene increases with the decrease of stereoregularity in EPR. The measured dimensions of the unit cell of a semi-crystalline polyethylene are not affected by the introduction of an amorphous component for PE(2)/EPR blends. According to the measurement of  $T_g$  by dynamic mechanical thermal analyzer, these blend systems were immiscible regardless of blend composition. The three blends showed a linear relationship in the density behavior with change of blend ratio. This trend means that there are very weak or no interactions between the two component chain segments. From the measurement of stress-strain behavior for these blends, the blend composition of 50/50 has the lowest breaking strength. In this paper, the research was carried out to examine crystallinity, interaction parameter, diluent effect, spherulite size in this three PE(2)/EPR blends.

## II. Experimental

### 1. Materials

PE(2) was obtained from hydrogenation of cis-polybutadiene (cis-PBD) (Goodyear, Budene 1208).

r-EPR (Vistalon 404) was supplied by Exxon Co.. alt-EPR was obtained from hydrogenation of cis-polyisoprene (Goodyear, Natsyn 2210). iso-alt-EPR was obtained from hydrogenation of isotactic-cis-poly(1,3-pentadiene) (Goodyear).

### 2. Blending

PE(2) was blended with r-EPR, alt-EPR, and iso-alt-EPR to investigate their mutual compatibility. Samples of various compositions were prepared by solution blending in a mutual solvent (*p*-xylene) followed by solvent evaporation. The evaporation of solvent from the blend solution was carried out at 90°C, and 25.4 cmHg in a vacuum drying oven to prevent precipitation of polyethylene due to crystallization.

### 3. Instruments and Sample Preparation

The melting points of polymer blends were measured by differential scanning calorimeter (DSC, Dupont 9900 thermal analyzer) with disc memory. DSC analyses were carried out for each polymer sample by placing approximately 10mg of sample into an aluminum sample pan. Crystalline spherulite morphologies in crystalline polymer blends were analyzed using SALS. The instrument uses a He-Ne laser light source with a wavelength of 6328 Å. The scattered intensity was monitored by a two-dimensional Vidicon detector interlinked with an optical multi-channel analyzer (OMA III, Model 1460, EG & G Princeton Applied Research Co.). A couple of heating cells were used for time evolution scattering studies; one was controlled at the experimental temperature while the other was used for preheating. Scattering patterns were obtained using Polaroid 55 photographic films with a Polaroid 545 film holder. A 2% polymer blend solution was prepared for solution cast samples. After solution blending, the solution was placed on a microscope slide in the dry oven at 90°C. Thin polymer films of 0.1mm thickness were collected after evaporation of the solvent.

### III. Results and Discussion

#### 1. Crystallinity

The heat of fusion ( $\Delta H_f$ ) for each composition of PE(2)/EPR blend systems was determined from the area under the melting transition as measured through DSC. The heats of fusions of the different PE/EPR blends are plotted in Figure 1 as a function of weight fraction of the amorphous component. Percent crystallinity was calculated by selecting the heat of fusion 100% crystalline PE as 70cal/g<sup>6</sup>. With increasing the rubber content, the percent crystallinity of the blend decreases in a linear fashion. In addition, as the stereoregularity in the EPR decreases, the level of crystallinity decreases at the same blend ratio. Generally speaking, the decrease in crystallinity with increasing concentration of the amorphous component is attributed to a decrease in the degree of annealing and/or a reduced diffusion rate. Both of these effects are known to cause a reduction in the rate and degree of crystallization. The difference with the type of blend may derive from the effect the stereoregularity in EPR. An *r*-EPR has the greatest mobility and the kinetics of diffusion in comparison with *alt*-EPR and *iso-alt*-EPR.

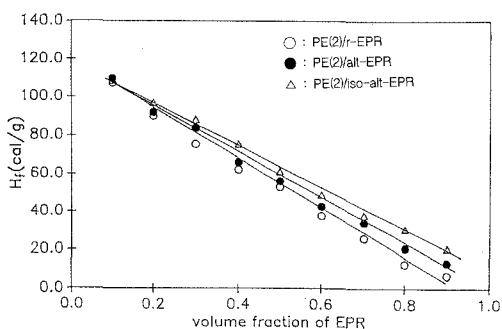


Figure 1. Observed heat of fusion for the three PE(2)/EPR blends.

#### 2. Interaction Parameter

The thermodynamic interaction parameters for the

*cis*-PBD/PE blends were obtained by analysis of the melting point depression. Nishi and Wang<sup>7</sup> extended Flory's theory of the melting point depression by using Scott's expression for a binary polymer blend system. The resulting expression from their analysis of crystalline and amorphous polymers leads to Equation (1).

$$\frac{1}{\Phi_1} \left( \frac{1}{T_m} - \frac{1}{T_m^0} \right) = - \frac{BV_3\Phi_1\chi_{23}}{\Delta H_m V_2} \quad (1)$$

where

$\Phi_1$  : Volume fraction of rubber content

$T_m$  : Absolute melting temperature

$T_m^0$  : Equilibrium melting temperature

$B$  : Interaction energy density characteristic of polymer pair

$V_2, V_3$  : Molar volume of polymer 2 and polymer 3

$\chi_{23}$  : Interaction parameter between polymer 2 and polymer 3

$\Delta H_m$  : Enthalpy change of mixing

From their studies on poly(vinylidene fluoride)/poly(methyl methacrylate) (PVF<sub>2</sub>/PMMA) and poly(vinylidene fluoride)/poly(ethyl methacrylate) (PVF<sub>2</sub>/PEMA) mixtures, a plot of  $\Delta T_m/\Phi_1 T_m$  versus  $\Phi_1 T_m$  had straight line with an intercept close to zero. Therefore, factors such as crystal imperfection and reduction in lamellar thickness were not considered to be major factors in the lowering of the melting point. Kwei and Frisch<sup>8</sup> further extended Nishi and Wang's treatment<sup>7</sup> by taking into account the morphological effects which may also contribute to the melting point depression. The numerical data of melting point in the *cis*-PBD/PE with blend ratio are listed in Table 1. The resulting analytical expressions are shown in Equation(2) and Equation(3).

$$\begin{aligned} \Delta H_u (T_m^0 - T_m) / \Phi_1 R T_m^0 - T_m / m_1 - \Phi_1 T_m / 2 m_2 \\ = C/R - b \Phi_1 \end{aligned} \quad (2)$$

$$x = a + b/T \quad (3)$$

where

- $\Delta H_u$  : Heat of fusion per mole of repeating unit of crystalline component  
 R : Gas constant  
 $m_1, m_2$  : Chain repeat lengths of polymer 1 and polymer 2  
 C : Proportionality constant  
 a, b : constants  
 T : Absolute temperature

**Table 1. Observed Melting Point of PE(2)/EPR Blends**

Composition EPR/PE(2)	$T_m$ (°C)		
	PE(2)/r-EPR	PE(2)/alt-EPR	PE(2)/iso-alt-EPR
10/90	118.7	119.2	119.1
20/80	118.1	118.5	118.6
30/70	117.0	117.8	118.1
40/60	116.6	117.4	117.2
50/50	115.4	116.2	117.1
60/40	114.3	115.1	116.9
70/30	113.3	114.7	116.6
80/20	112.6	114.0	116.2
90/10	111.2	113.7	115.7

**Table 2. Calculated Thermodynamic Interaction Parameter ( $\chi$ ) and C/R for the Three Blends from  $T_m$  Measurements**

Polymer Blend	C/R*	Slope (° K)	$\chi$ (at $T_m$ )	$\chi_{cr}$
PE(2)/r-EPR	8.59	0.31	0.0003	0.012
PE(2)/alt-EPR	5.91	0.05	0.0001	0.016
PE(2)/iso-alt-EPR	3.86	0.15	0.0004	0.027

From a plot of the left hand side of Equation(2) vs.  $\Phi_1$ , they found a non-zero intercept for poly(phenylene oxide)/polystyrene (PPO/PS) blends, an intercept value was found to increase with decreasing PS molecular weight. The authors concluded that the melting point depression was linked to the diluent effect and the morphological effect. In this study, the melting point data for each cis-PBD/PE mixture were plotted in accordance

with Equation(2). A value of  $\Delta H_u=70\text{cal/g}$ (980cal per mole of  $-\text{CH}_2-$  unit) which was reported by Schultz<sup>6</sup>, is used in this analysis. The values of the interaction parameter,  $\chi$ , for the polymer blends were obtained by using a linear regression analysis on the data of Table 1. The parameters C/R and b were determined from the intercept and slope values, respectively. The calculated values for the interaction parameter based on the depression of the melting point, as well as the critical interaction parameter determined using Equation(4) are listed in Table 2.

$$(\chi_{ab})_{cr} = \frac{1}{2} \left[ \frac{1}{X_a^{1/2}} + \frac{1}{X_b^{1/2}} \right]^2 \quad (4)$$

Where  $(\chi_{ab})_{cr}$  is the critical interaction parameter between polymer a and b,  $X_a$  and  $X_b$  are the degree of polymerization in polymer a and b. The results indicate that the measured interaction parameters for the different blend systems are all about  $1 \times 10^{-3} \sim 2 \times 10^{-3}$ . Since the value of the slope is quite small and close to zero, it may be concluded that the interaction parameter is also close to zero. In addition, no systematic dependence appears to exist between the interaction parameter and the stereoregularity of EPR. This suggests that three kinds of EPR's studied here have the same net thermodynamic interaction effect with PE(2) and that this net interaction is close to zero. The intercepts from the above plots are equal to C/R which is one linear function of the lamellar thickness. Based on the observation that the crystallinity of the PE(2)/EPR blend decreased with stereoregularity of the EPR component, one may conclude that these effects are due to decreasing crystallinity in the following order: r-EPR<alt-EPR<iso-alt-EPR. This implies that the morphological effect on the melting point depression increases in order of r-EPR<alt-EPR<iso-alt-EPR. Lin<sup>9</sup> found the same result for blend of different ethylene content EPR's with LDPE. He observed that in the blend with LDPE, high ethylene content EPR has

melting point depression, low crystallinity, and large C/R value.

### 3. Diluent Effect

Besides the calculation of an interaction parameter, one series of additional experiments was conducted to investigate further the influence of EPR on the melting behavior of PE(2) and the experimental technique of melting point analysis. Melting point was measured after an isothermal crystallization from the molten state. Experiments were carried out after cooling the sample from the melt state to a predetermined crystallization temperature below  $T_m$  for 10 minutes using DSC. A plot of the crystallization temperature,  $T_c$ , versus observed melting point,  $T_m$ , was then drawn. For binary polymer blends, the dependence on composition can be more complicated than that observed for homopolymers. For those polymers which exhibit a melting point depression, the three fundamental types of behavior were illustrated in Figure 2<sup>10</sup>. Various materials have been found to display a phase behavior similar to that illustrated. In case I,  $T_m$  is found to increase linearly with  $T_c$ . This type of behavior is often observed in semicrystalline homopolymers. The slope of the straight line is independent of composition and of  $T_c$ . As the concentration of the crystallizable component decreases, the extrapolation value of  $T_m$  also decrease (Figure 2A). In case II,  $T_m$  of the blend increases linearly with  $T_c$ , but the lines extrapolate to the same equilibrium  $T_m$  value of the homopolymer and their slopes depend on composition (Figure 2B). In case III,  $T_m$  is a linear function of  $T_c$  only for a certain interval of  $T_c$ . Thereafter a nonlinear trend is observed at high crystallization temperatures and the actual depression values are small and not dependent on composition (Figure 2C). The depression of the melting point for blends belonging to case I has been interpreted as being due to a diluent effect of the amorphous component. According to Hoffman<sup>11</sup>, a plot of the melting

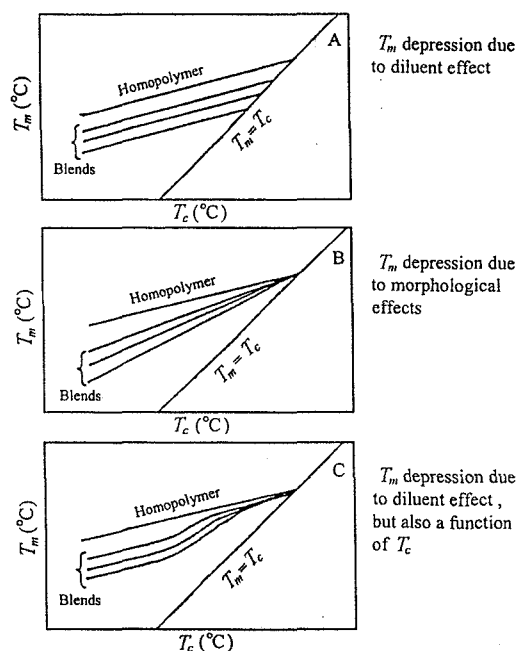


**Figure 2.** Schematic illustration of possible  $T_m$  vs.  $T_c$  behavior for semi-crystalline blends.

temperature  $T_m$  of the crystals against their crystallization temperature gives a straight line in accordance with the Equation(5).

$$T_m = T_m^0(1 - \gamma^{-1}) + \gamma^{-1}T_c \quad (5)$$

Where  $\gamma$  is a morphological factor that turns out to be almost independent of composition and chemical structure. The Systems showing case I behavior include of PVF<sub>2</sub>/PMMA<sup>7</sup>, PVF<sub>2</sub>/PEMA<sup>12</sup>, and isotactic-polypropylene/ethylene-propylene rubber<sup>13</sup>. These systems have shown a linear type behavior with respect to composition. Paul and Altamiano<sup>14</sup> and Natov et al.<sup>15</sup> interpreted case II due to morphological effects. These effects are considered results from the formation of smaller and less perfect crystallites by the addition of a non-crystallizable component especially. Blends of poly(ethylene oxide)/poly(methyl methacrylate) show a behavior similar to that for case III. This latter type of behavior has been interpreted by

Martuscelli and Demma<sup>16</sup> due to the occurrence of phase separation. For low  $T_c$  ( the linear part of the  $T_m$ - $T_c$  plot) the two components are completely miscible in the melt, and the non-crystallizing component acts as a diluent. At higher  $T_c$  the mutual solubility of the components decreases giving rise

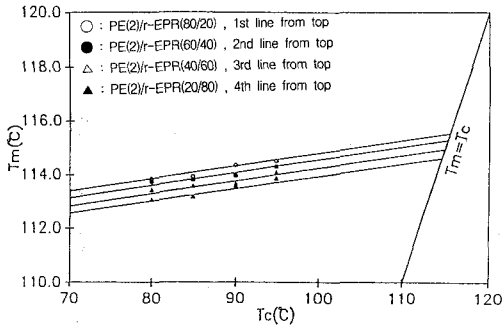


Figure 3. Observed melting point temperature vs.  $T_c$  for PE(2)/r-EPR.

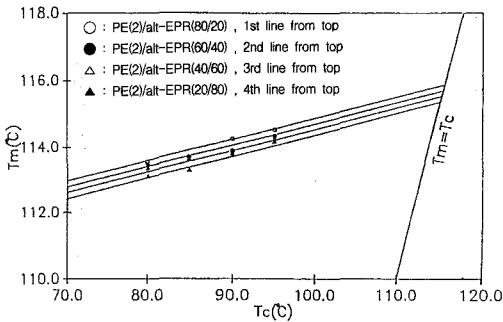


Figure 4. Observed melting point temperature vs.  $T_c$  for PE(2)/alt-EPR

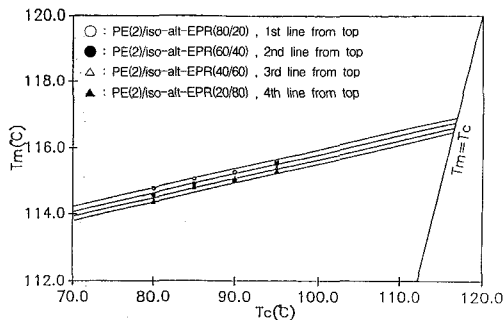


Figure 5. Observed melting point temperature vs.  $T_c$  for PE(2)/iso-alt-EPR

to the formation of a two-phase system. As shown in Figures 3 to 5, the Hoffman- Weeks correlations were linear and identical to those of the PE(2)/EPR blend. This type of blends show the diluent effect of EPR's on PE(2). The Flory interaction parameter ( $\chi$ ) must thus zero or slightly positive for these blends.

#### 4. Spherulite Size

Small angle light scattering was employed to study the spherulite morphology of the different PE(2)/EPR blends. The He-Ne light scattering patterns for the various solution cast mixtures are obtained. The determination of the spherulite radius( $R_s$ ) by SALS can be found from Equation(6).

$$U_{\max} = 4.1 = 4 \pi (R_s / \lambda') \sin(\theta_{\max} / 2) \quad (6)$$

Where  $U_{\max}$  is the shape factor at maximum intensity,  $\lambda'$  is the wavelength of light in the medium, and  $\theta$  is the radial scattering angle. According to Equation(6), an inverse relationship exists between the angle of maximum scattering intensity ( $\theta_{\max}$ ) and the spherulite size. The angle of the maximum scattering intensity was determined using an optical densitometer. The average spherulite size calculated was plotted against the volume fraction of EPR and are shown in Figure 6. These results suggest that an increasing concentration of the amorphous content. It is well known, that the average size of a spherulite is inversely proportional to the nucleation rate in semi-crystalline homopolymers. Similarly, the observed spherulite size for a blend can be attributed to differences in the rate of nucleation, and thus enhances the size of spherulite. With respect to chain architecture, i.e., the stereoregularity, the increase in spherulite size is observed with decreasing the stereoregularity of EPR. This result arises from a melting point depression associated with the stereoregularity of EPR in the blend, as discussed in Table 1 earlier. The supercooling temperature increases as the stereoregularity of EPR

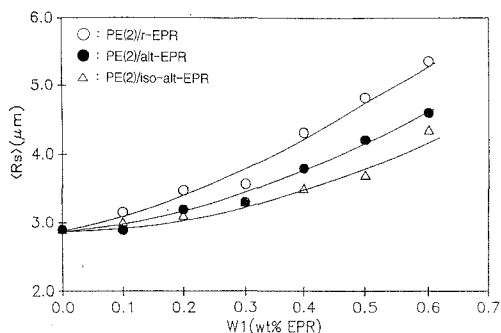


**Figure 6.** Plot of spherulite size vs. composition for different PE(2)/EPR blends.

is decreased. The increase in the average spherulite size is followed by decreasing the rate of nucleation.

#### IV. Conclusion

The crystallinity of PE(2) decreases with increasing amorphous content, EPR, by a decrease in both the degree of annealing and rate of diffusion of the crystallizable polymer content. In the three blend systems, the crystallinity decreases with and blend composition. The thermodynamic interaction parameter,  $\chi$ , for different binary polymer mixture was determined by an analysis of the phase diagram near the melting point. The PE(2)/EPR blends showed a value for the interaction parameter approximately equal to zero. As a result, these blend systems were determined to be miscible on a molecular scale near or above the crystalline melting point of the crystallizable component. From the measurement of  $T_m$  vs.  $T_c$  behavior for line in a plot of  $T_m$  vs.  $T_c$ , the result implies that the diluent effect of amorphous component have on semi-crystalline PE(2). The spherulite size depended upon

blend composition and stereoregularity of EPR because all three blends bring a change in the supercooling nucleation. Although an increase in the spherulite size is observed, the degree of spherulite perfection is decreased.

#### References

1. U. R. Cho, *Elastomer*, **36**, 3, 169 (2001).
2. U. R. Cho, *Polymer(Korea)*, **19**, 515 (1995).
3. U. R. Cho, *Polymer(Korea)*, **19**, 535 (1995).
4. U. R. Cho, *Korea Polym. J.*, **7**, 196 (1999).
5. U. R. Cho, *Korea Polym. J.*, **8**, 66 (2000).
6. J. Schultz, "Polymer Materials Science", Prentice Hall, Inc., New Jersey (1974).
7. T. Nishi and T. Wang, *Macromol.*, **8**, 909 (1975).
8. T. Kwei and H. Frisch, *Macromol.*, **11**, 1267 (1978).
9. W. Y. Lin, Ph. D. Dissertation, Univ. of Akron. (1983).
10. G. Allegra and I. Bassi, *Adv. Polym. Sci.*, **6**, 549 (1969).
11. J. D. Hoffman, *Soc. Plast. Eng. Trans.*, **4**, 315 (1964).
12. T. Kwei, G. Patterson and T. Wang, *Macromol.*, **9**, 780 (1976).
13. E. Martuscelli, C. Silivestre and G. Abate, *Polymer*, **23**, 229 (1982).
14. D. Paul and J. Altaminano, *Am. Chem. Adv. Chem. Ser.*, **142**, 371 (1975).
15. M. Natov, L. Peava and E. Djararova, *J. Polym. Sci. Part C*, **16**, 4197 (1973).
16. E. Martuscelli and G. Demma, "Polymeric Blends : Processing-Morphology and Properties", ed., E. Martuscelli, R. Palumbo and M. Kryszevski, Plenum Press, N.Y. (1982).